Science
AAAS

The Closing Door of Climate Targets

Thomas F. Stocker

Science **339**, 280 (2013);
DOI: 10.1126/science.1232468

the action of glucocorticoid and mineralocorticoid (a steroid hormone so-named because it controls fluid homeostasis) receptors in diverse functions is a dependence on other mediators and ongoing cellular processes. For example, activation of these receptors in the brain is associated with the release of the neurotransmitter glutamate (*8*–*10*) as well as the release of endocannabinoids, lipids that modulate appetite, mood, and memory (*11*, *12*). These hormones also act on receptors that translocate to the mitochondria to control calcium buffering (*13*). Glucocorticoids support neuronal synapses (*14*), dendritic growth (*15*), and neuronal plasticity (*16*), suggesting a role in maintaining a dynamic brain architecture. Moreover, glucocorticoid action on some processes involves concurrent activity of other mediator systems, such as oxytocin for neurogenesis (*17*) and adrenergic mechanisms for learning (*18*).

Clearly, our understanding of the complex and widespread actions of adrenal steroid hormones throughout the developing and adult nervous system is at an early stage. The finding that these hormones play a role in the discrete specification of neuronal circuits in the brain and behavioral outcomes point to potential therapeutic approaches that could intervene and restore normal behaviors.

References and Notes

1. J. Barik *et al.*, *Science* **339**, 332 (2013).
2. M. Niwa *et al.*, *Science* **339**, 335 (2013).
3. F. Ambroggi *et al.*, *Nat. Neurosci.* **12**, 247 (2009).
4. A. Crudo *et al.*, *Endocrinology* **153**, 3269 (2012).
5. X. Yang *et al.*, *Biochem. Biophys. Res. Commun.* **420**, 570 (2012).
6. A. F. Schatzberg, A. J. Rothschild, *Ann. N.Y. Acad. Sci.* **537**, 462 (1988).
7. K. R. Yamamoto, *Annu. Rev. Genet.* **19**, 209 (1985).
8. M. Popoli, Z. Yan, B. S. McEwen, G. Sanacora, *Nat. Rev. Neurosci.* **13**, 22 (2012).
9. H. Karst *et al.*, *Proc. Natl. Acad. Sci. U.S.A.* **102**, 19204 (2005).
10. E. M. Prager, L. R. Johnson, *Sci. Signal.* **2**, re5 (2009).
11. M. N. Hill, B. S. McEwen, *Prog. Neuropsychopharmacol. Biol. Psychiatry* **34**, 791 (2010).
12. J. G. Tasker, S. Di, R. Malcher-Lopes, *Endocrinology* **147**, 5549 (2006).
13. J. Du *et al.*, *Proc. Natl. Acad. Sci. U.S.A.* **106**, 3543 (2009).
14. C. Liston, W. B. Gan, *Proc. Natl. Acad. Sci. U.S.A.* **108**, 16074 (2011).
15. E. Gould, C. S. Woolley, B. S. McEwen, *Neuroscience* **37**, 367 (1990).
16. M. Spolidoro *et al.*, *Nat. Commun.* **2**, 320 (2011).
17. B. Leuner, J. M. Caponiti, E. Gould, *Hippocampus* **22**, 861 (2012).
18. S. Okuda, B. Roozendaal, J. L. McGaugh, *Proc. Natl. Acad. Sci. U.S.A.* **101**, 853 (2004).

10.1126/science.1233713

CLIMATE CHANGE

The Closing Door of Climate Targets

The linear relationship between cumulative carbon emissions and global climate warming implies that as mitigation is delayed, climate targets become unachievable.

Thomas F. Stocker

Robust evidence from a range of climate–carbon cycle models shows that the maximum warming relative to pre-industrial times caused by the emissions of carbon dioxide is nearly proportional to the total amount of emitted anthropogenic carbon (*1*, *2*). This proportionality is a reasonable approximation for simulations covering many emissions scenarios for the time frame 1750 to 2500 (*1*). This linear relationship is remarkable given the different complexities of the models and the wide range of emissions scenarios considered. It has direct implications for the possibility of achieving internationally agreed climate targets such as those mentioned in the Copenhagen Accord and the Cancun Agreements (*3*, *4*). Here I explain some of the implications of the linear relationship between peak warming and total cumulative carbon emissions.

The considerations presented here are based on the assumption of a generic set of carbon dioxide emissions scenarios that reasonably approximate what is presently observed and what needs to be done to limit warming below a specific global mean temperature increase. In these idealized and illustrative emissions scenarios (see the Box), emissions follow an exponential increase with a constant rate until a given year, after which the emissions decrease exponentially at a constant rate. The scenarios delineate the boundaries for any discussion and decision process for global measures limiting anthropogenic climate change.

Results from a large number of Earth system model simulations suggest that peak warming, ΔT, and cumulative CO_2 emissions, C_∞, are nearly linearly related via the parameter β, which is the peak response to cumulative emissions (see Eq. 3 in the Box).

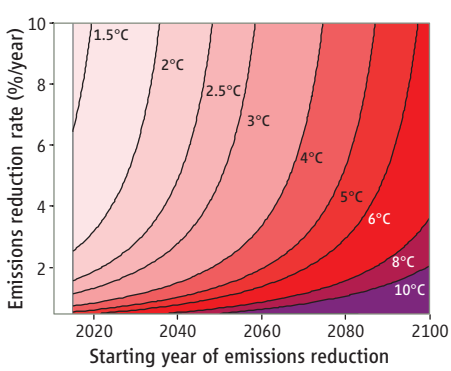

Contours of peak warming. Contours of peak CO_2-induced warming (as given by Eq. 3 in the Box) as a function of the starting date of the GMS and the implemented reduction rate of emissions. Parameters are $C_0 = 530$ GtC, $E_0 = 9.3$ GtC per year, $\beta = 2°C$ $(TtC)^{-1}$, and $r = 1.8\%$ per year. The later the GMS starts, the higher the required emissions reduction rate is for a given peak warming.

The value of β is estimated to be between 1.3° and 3.9°C per trillion metric tons of carbon (1 TtC = 10^{18} g carbon) (*1*). The uncertainty in β arises from the range of climate sensitivities and carbon cycle feedbacks in the models. More recent estimates of a closely related quantity, the transient climate response to cumulative emissions, take into account observational constraints and report 1.0° to 2.1°C $(TtC)^{-1}$ (*2*). However, this quantity is less useful here because warming can still continue when emissions stop. This warming is better captured by the peak response to cumulative emissions.

For a given β, the peak warming is determined by three quantities in these simple scenarios: the current rate of emissions increase, the starting time of the Global Mitigation Scheme (GMS), and the rate of emissions reduction realized by the GMS. The latter two depend on future choices and are therefore policy-relevant. As shown in the first figure, a delay in the start of the GMS results in a rapid increase in ΔT as a result of the continued exponential increase in emissions before the start of mitigation. Likewise, for a given starting date of mitigation, achieving a low climate target calls for very aggressive emission decreases. For example, under the present illustrative assumptions, keeping CO_2-induced global warming below 2°C would require emissions reductions of almost 3.2% per year from 2020 onward; this is more than

Climate and Environmental Physics, Physics Institute, and Oeschger Centre for Climate Change Research, University of Bern, 3012 Bern, Switzerland. E-mail: stocker@climate.unibe.ch

A set of simple analytic greenhouse gas emissions scenarios

For simplicity, we assume that past greenhouse gas emissions followed an exponential path, which is a reasonable approximation for historical emissions (*6*). To extract some essential characteristics and consequences of increasing emissions followed by sustained mitigation, we construct a simple emission path that consists of two exponentials,

$$E(t) = \begin{cases} E_0 \cdot e^{r\cdot(t-t_0)} & t_0 < t \le t_1 \\ E_0 \cdot e^{r\cdot(t_1-t_0)} \cdot e^{-s\cdot(t-t_1)} & t > t_1 \end{cases} \quad (1)$$

where $E(t)$ are the anthropogenic CO_2 emissions at time t, E_0 = 9.3 GtC year^{-1} is the emission at t_0, taken here as the year 2009 (*7*), and r is the rate of emissions increase per year until time t_1. The exact path of emissions before t_0 is not important here, because its effect can be taken into account by the cumulative emissions until t_0, C_0. We select C_0 = 530 GtC (*6*). A Global Mitigation Scheme (GMS) starts at time t_1 with emissions reductions at the constant rate of s. We take r = 1.8% per year, which is somewhat lower than a recent estimate of r (*6*) for the entire historical period, in order to be more consistent with the cumulative emission until 2009 as also estimated by (*6*). Similar peak-and-decline emissions trajectories represented by analytical functions were used recently (*8*), with a smooth transition path to sustained emissions reductions.

The scenario path for $t > t_1$ in Eq. 1 implies that negative emissions (active removal of carbon from the atmosphere) on a global scale will not be realized anytime in the future. This should be considered as a conservative, but likely realistic, assumption. The total cumulative emissions C_∞ follow from Eq. 1 and are given by

$$C_\infty = C_0 + \int_{t_0}^{+\infty} E(t)dt = C_0 + E_0 \cdot \left(\tfrac{1}{r} + \tfrac{1}{s}\right) \cdot e^{r\cdot(t_1-t_0)} - \tfrac{1}{r}E_0 \quad (2)$$

This simple scenario can be used to illustrate some fundamental and policy-relevant consequences of the robust linear relationship between peak warming and cumulative emissions. I consider implicitly only long-lived greenhouse gases, which is appropriate unless temperatures peak in the next few decades.

Simulations with many Earth system models (*1*, *2*) show a near-linear relationship between peak warming, ΔT, and cumulative CO_2 emissions, C_∞,

$$\Delta T = \beta \cdot C_\infty \quad (3)$$

where β is the factor of proportionality between cumulative emissions and peak warming and is referred to as the peak response to cumulative emissions.

By taking in Eq. 2, the limit of $s = \infty$, and using Eq. 3, one obtains

$$\Delta T_{min} = \beta \cdot \left(C_0 + \tfrac{1}{r}E_0 \cdot (e^{r\cdot(t_1-t_0)} - 1)\right) = \beta \cdot C_1 \quad (4)$$

which is the minimum peak warming resulting from the most aggressive GMS, that is, zero emissions from time t_1 onwards. Achievable climate targets are therefore determined by the cumulative emissions until time t_1, C_1.

doubled if GMS starts in 2032. Thus, every year counts; if mitigation actions are delayed, much larger emissions reductions are later required to maintain a selected target.

The simple emission pathway provides another important insight. If we assume that the most aggressive GMS is "zero emission" (that is, carbon will not be extracted actively from the atmosphere), the total amount of carbon emitted up to the start of GMS determines the lowest peak warming, or minimum climate target, ΔT_{min} (see Eq. 4 in the Box). An absolute limit then emerges in the climate system for the possibility of satisfying a climate target. Past cumulative emissions up to the time of sustained emissions reductions leave a legacy, or commitment, in the future, irrespective of any long-term mitigation efforts. As the starting time of GMS is delayed, the low climate targets are progressively lost. The door for these climate targets closes irreversibly (see the second figure, panel A).

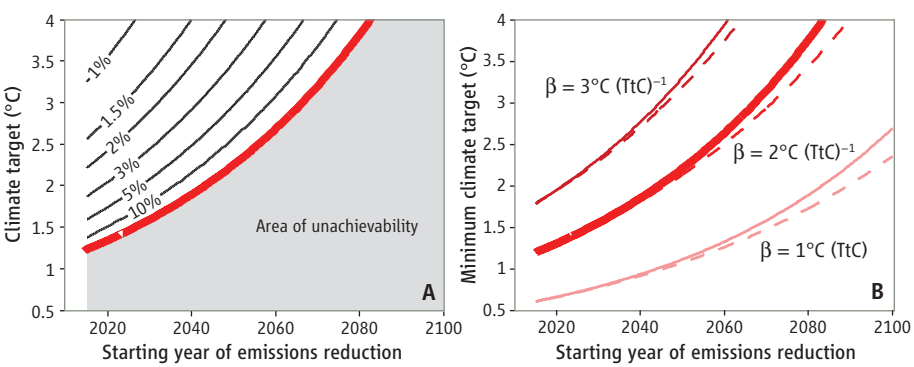

A closing door. (**A**) Contours of required emissions reduction rate s (% per year), derived from Eq. 3, as a function of the starting date of the GMS and the desired climate target. The red line indicates the achievable minimum climate target as a function of the starting date as given by Eq. 4. Climate targets increase exponentially with later starting years of the GMS and become unachievable in the gray shaded area. Parameters are as in the first figure. (**B**) Achievable minimum climate target for three values of the peak response to cumulative emissions, β, and the rate of emissions increase used in the first figure (solid curves, r = 1.8% per year), and a lower rate of emissions increase roughly representative of the past 10 years, r = 1.5% per year (dashed curves). Higher values of β imply higher peak warming.

Under the present illustrative assumptions, the 1.5°C target expires after 2028, and the 2°C target vanishes after 2044. These times would be later if a period of stabilized emissions preceded the GMS. The more likely situation, however, is that a specific climate target becomes unreachable much earlier, because there are upper limits on sustained emissions reduction rates imposed by what the countries' economies can realize collectively given the present state of technology and infrastructure.

Economic models estimate that feasible maximum rates of emissions reduction may not exceed about 5% per year (*5*). Under this assumption, the 1.5°C target has become unachievable before 2012, the 2°C target will become unachievable after 2027, and the 2.5°C target will become unreachable after 2040.

These years are only illustrative of the finite time that climate targets remain available options in the presence of continued greenhouse gas emissions. Uncertainties in β, or in the rate of emissions increase, do not change the overall findings (see the second figure, panel B). But it is clear that reducing uncertainties in the quantity β, which com-

Published by AAAS

bines climate sensitivity and carbon cycle feedbacks (*2*), is most important for a more reliable estimate of which climate targets are still achievable.

As the emissions scenarios considered here illustrate, even well-intentioned and effective international efforts to limit climate change must face the hard physical reality of certain temperature targets that can no longer be achieved if too much carbon has already been emitted to the atmosphere. Both delay and insufficient mitigation efforts close the door on limiting global mean warming permanently. This constitutes more than a climate change commitment: It is the fast and irreversible shrinking, and eventual disappearance, of the mitigation options with every year of increasing greenhouse gas emissions.

References and Notes

1. M. R. Allen *et al.*, *Nature* **458**, 1163 (2009).
2. H. D. Matthews, N. P. Gillett, P. A. Stott, K. Zickfeld, *Nature* **459**, 829 (2009).
3. UNFCCC, The Copenhagen Accord, FCCC/CP/2009/11/Add.1 (United Nations Framework Convention on Climate Change, 2009).
4. UNFCCC, The Cancun Agreements, FCCC/CP/ 2010/7/Add.1 (United Nations Framework Convention on Climate Change, 2010).
5. M. den Elzen, M. Meinshausen, D. van Vuuren, *Glob. Environ. Change* **17**, 260 (2007).
6. R. J. Andres *et al.*, *Biogeosciences* **9**, 1845 (2012).
7. P. Friedlingstein *et al.*, *Nat. Geosci.* **3**, 811 (2010).
8. N. H. A. Bowerman *et al.*, *Philos. Transact. A Math. Phys. Eng. Sci.* **369**, 45 (2011).

Acknowledgments: M. Allen is acknowledged for critical and thoughtful comments.

Published online 29 November 2012

10.1126/science.1232468

PLANETARY SCIENCE

A Wet and Volatile Mercury

Observations by the MESSENGER spacecraft are revealing details of Mercury's dynamic atmosphere.

Paul G. Lucey

One of the more startling discoveries in planetary science was that the poles of Mercury feature deposits that are extremely bright at radar wavelengths (*1*), interpreted to be due to the presence of thick water ice. Because Mercury's rotation axis is almost normal to the plane of its orbit, the temperature of polar craters largely or completely shaded from the Sun should be very low. On the Moon, for example, where the rotation axis tilt is similarly small, the polar temperatures in permanently shadowed regions have been measured by infrared radiometry to be as low as 25 K (*2*). These topographic depressions might be expected to contain cold-trapped volatile material that might be introduced by comets, water-bearing asteroids, or other sources. On pages 292, 300, and 296 of this issue, Lawrence *et al*. (*3*), Paige *et al*. (*4*), and Neumann *et al*. (*5*) report on the latest results from the MESSENGER (MErcury Surface, Space ENvironment, GEochemistry, and Ranging) mission confirming the expectations that the atmosphere of Mercury is indeed a wet volatile one, as well as providing the odd surprise.

Compounds other than water ice have been suggested to account for the radar observations, with sulfur being of particular interest given the extremely high temperatures of equatorial Mercury and the abundant evidence for volcanic activity on the small planet (*6*). However, Lawrence *et al*. report depressed neutron fluxes at Mercury's north pole and show that only high concentrations of hydrogen confined to the known radar-bright locations are consistent with the neutron flux measured at both high and intermediate energies. Thermal modeling supports their conclusion. Paige *et al*. apply a thermal model of the polar Moon to polar Mercury to estimate the surface and shallow subsurface temperatures, supported by detailed topography measured by the MESSENGER laser altimeter and validated with lunar remote radiometric measurements. They find that the radar-bright areas are almost exclusively confined to places where shallow subsurface temperatures hover near 100 K or less, and owing to the exponential dependence of volatility on temperature, water is the only compound with the right volatility and cosmochemical abundance to account for the radar anomalies. On the other hand, maximum temperatures experienced by most of these radar-bright regions are too high to sustain surface ice, so that if ice is responsible for the radar features, it must be buried by a few centimeters of insulating material, such as dry Mercury soil.

These results fulfilled promises made by the MESSENGER scientists that Mercury's enigmatic polar volatile would be identified. But polar measurements contained a major surprise. The laser altimeter carried on the spacecraft, which provided the topographic measurements enabling the detailed thermal modeling, also measured the reflectance of Mercury's surface in the unilluminated polar regions. This instrument compares the strength of the outgoing laser pulse to the return power, normalized to the range to the surface. Pioneered on Mars and the Moon, this method measures the normal albedo of the surface without the influence of local topography or the need for solar illumination, which is weak or absent at the poles. Before MESSENGER's arrival at Mercury, it was anticipated that bright surface deposits of ice or sul-

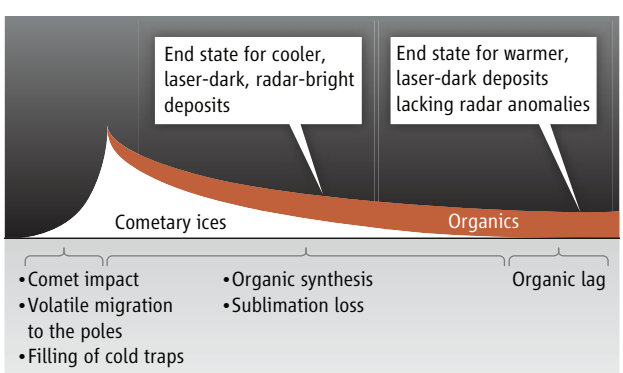

Atmosphere dynamics. Mercury's polar cold traps appear to have been filled by one or more comet impacts that introduced massive quantities of water and other volatile vapors in the tenuous atmosphere that promptly migrated to the polar cold traps. Ices began to immediately sublimate, and to acquire organic lag deposits, probably from radiation-induced chemical synthesis. The colder parts of the poles now exhibiting radar anomalies retained water ice below the lag deposit, while in warmer portions the ice entirely sublimed away, leaving the low-reflectance organic residue. Not depicted are the rare very-high-reflectance spots that are confined to the coldest portions of the pole. These may indicate a slow continuous production of water from small wet meteorites, solar wind proton interactions with oxygen in Mercury's surface, or inhibition by the very low temperatures of the organic synthesis occurring elsewhere.

Hawaii Institute of Geophysics and Planetology, University of Hawaii, 2525 Correa Road, Honolulu, HI 96822, USA. E-mail: lucey@higp.hawaii.edu